

*Full Length Research Paper*

## Influence of etching on the optical properties of a-plane-oriented ZnO epilayers grown by plasma-assisted molecular beam epitaxy

Bassirou, L. O.

Université Cheikh Anta Diop, Dakar, Senegal.

Received 20 October, 2015; Accepted 24 November, 2015

**A-plane-oriented ZnO epilayers grown by plasma-assisted molecular beam epitaxy were studied with respect to their optical properties. 10K-photoluminescence (PL) and reflectivity were used to analyze various 2  $\mu\text{m}$ -thick ZnO films etched at different etching profile. The PL spectra show the band emission of the structures become narrower when the etching profile increase. At 0.75  $\mu\text{m}$  etching profile, two structures at 3.38 eV corresponding to the A-free exciton transition and at 3.41 eV corresponding to the B-free exciton transition and the Y line were observed in the 10K PL spectrum providing that the optical properties of the ZnO sample are preserved and enhanced.**

**Key words:** Excitonic, photoluminescence, wet-chemical etching, a-plane ZnO.

### INTRODUCTION

As a wide bandgap ( $E_g=3.37$  eV) semiconductor, ZnO has attracted considerable attention due to its potential applications, such as ultraviolet light-emitting devices and laser devices (Zhang et al., 2002). Compared with other wide bandgap materials, ZnO has a larger exciton binding energy (60 meV) (Zhang et al., 2002; Look, 2001), which paves the way for an intense near band edge excitonic emission at room (Bagnall et al., 1997) and even higher temperatures. A notable discovery in ZnO thin film materials is the observation of the ultraviolet (UV)-stimulated emission induced by the exciton-exciton scattering at moderate pumping intensity (Yu et al., 1997;

Cao, 1998). These results show that ZnO is a suitable candidate for optoelectronic device applications in the ultraviolet region. To obtain an efficient and stable UV exciton emission from ZnO films, it is necessary to know the energy band structure of ZnO. The development of thin-film etching processes is critical for device fabrication. It has been reported that ZnO thin films can be etched with both acidic and alkaline solutions including mixtures, such as  $\text{HNO}_3$ , HCl, HBr, BOE, BHF, and ammonia (Ito et al., 1995; Maki et al., 2002; Jingchang et al., 2007). Lou et al. (1997) reported that for radio-frequency magnetron-sputtered ZnO films, a 30 to

E-mail: lobass57@gmail.com.

Author(s) agree that this article remain permanently open access under the terms of the [Creative Commons Attribution License 4.0 International License](https://creativecommons.org/licenses/by/4.0/)

**Table 1.** Etching rate of different etchants and concentration.

Etching solution	Solution concentration	Etching rate ( $\mu\text{m}/\text{min}$ )
HCl : H <sub>2</sub> O	1: 60	1.9
HCl : H <sub>2</sub> O	1:200	0.9
HCl : H <sub>2</sub> O	1:500	0.4
HCl : H <sub>2</sub> O	1:900	0.2
HNO <sub>3</sub> : H <sub>2</sub> O	1:100	0.9
BOE*	1:7	0.06
H <sub>3</sub> PO <sub>4</sub> : C <sub>6</sub> H <sub>8</sub> O <sub>7</sub> : H <sub>2</sub> O	1:1:30	2.2
H <sub>3</sub> PO <sub>4</sub> : C <sub>6</sub> H <sub>8</sub> O <sub>7</sub> : H <sub>2</sub> O	1:5:60	1.8
H <sub>3</sub> PO <sub>4</sub> : C <sub>6</sub> H <sub>8</sub> O <sub>7</sub> : H <sub>2</sub> O	1:1:80	1.4
H <sub>3</sub> PO <sub>4</sub> : C <sub>6</sub> H <sub>8</sub> O <sub>7</sub> : H <sub>2</sub> O	1:1:150	1.0
H <sub>3</sub> PO <sub>4</sub> : C <sub>6</sub> H <sub>8</sub> O <sub>7</sub> : H <sub>2</sub> O	1:1:200	0.8
H <sub>3</sub> PO <sub>4</sub> : C <sub>6</sub> H <sub>8</sub> O <sub>7</sub> : H <sub>2</sub> O	1:1:300	0.6

45° etching slope downward with respect to the wafer plane was generated by acid-based, wet-chemical etching. Chang et al. (1992) indicated that strong acid (HCl) etching of sputtered ZnO films is uncontrollable, and ammonium chloride (NH<sub>4</sub>Cl) may be a suitable etchant with prior oxygen plasma treatment. Effects of the etching on the optical properties of ZnO have been studied by some authors. Zheng et al. (2002) studied ZnO nanowire by means of transmission electron microscopy, Raman spectrum, scanning electron microscopy and photoluminescence. Ipa et al. (2003) reported on the evolution of surface morphology, surface composition and PL intensity as a function of energy during etching of ZnO film. Zhu et al. (2004) have studied the optimized process of wet-chemical etching of a ZnO film grown on an r-plane sapphire substrate. Jong-Chang Woo et al. (2011) reported on the damage on the surface of zinc oxide thin films etched in Cl-based gas chemistry and Fernandez et al. (2011) have studied the high quality textured ZnO. Recently, Sun et al. (2014) reported on the pH-controlled selective etching of Al<sub>2</sub>O<sub>3</sub> over ZnO; Brenner et al. (2014) tested etch-resistant Zn<sub>1-x</sub>Mg<sub>x</sub>O alloys as an alternative to ZnO for carboxylic acid surface modification. Prasad et al. (2013) reported on ZnO etching and micro tunnel fabrication for high-reliability MEMS acoustic sensor and Ching et al. (2013) have studied the fabrication of porous zinc oxide by wet chemical etching and examined the structural and optical properties. However, detailed information regarding the optical properties of a-plane ZnO etched films has not been reported yet. Furthermore, the available results are mainly from polycrystalline or epitaxial (0001) ZnO films. It is necessary to investigate after etching the optical properties of the ZnO films. For these reasons, in the paper, we report on the optical properties of wet etching a-plane ZnO films. As the c-axis of the film lies in the surface, there exists unique in-plane anisotropy in

electrical and optical properties which can be used for novel device applications. The selection rules for optical transitions impose that A and B excitons have large oscillator strength for  $E_{\perp}c$  ( $c$  represents a crystal axis) and the C exciton for  $E//c$  polarization. The optical spectroscopy of a grown a-plane ZnO film was studied in detail elsewhere (Ding et al., 2012; Liang, 2010; Han, 2011).

## MATERIALS AND METHODS

Zinc oxide films with different thicknesses were epitaxially grown on an r-plane sapphire substrate by MBE at temperature  $T_g < 500^\circ\text{C}$ . The growth was performed using solid-source Zn and a RF-activated plasma as the oxygen source. The growth rate was 0.2  $\mu\text{m}/\text{h}$ ; slightly lower than the optimal growth rate in a  $c$ -direction growth. Prior to growth, the  $r$ -plane (01–12) sapphire substrates were thermally cleaned and subsequently exposed to oxygen plasma during 5 to 10 min. The growth process was *in situ* monitored by reflection high energy electron diffraction (RHEED) and a streaky RHEED pattern was maintained throughout the growth, albeit with a slight modulation in the [1–100] azimuth. *Ex situ* surface morphology was investigated by means of atomic force microscopy (AFM). The structural properties were investigated by high-resolution X-ray diffraction (HRXRD) experiments in high-resolution mode. Transmission electron microscopy (TEM) investigations were carried out in a JEOL 2010F field emission gun microscope. The results of these investigations are shown in a previous paper (Chauveau et al., 2007). Different etching solutions have been tested to etch the a-plane ZnO films as shown in Table 1.

It has been found that phosphoric acid, with suitable concentration, generates sharp pattern-edge slopes based on its relatively weak acidity and the diffusion-controlled etching mechanism. So we carry out optical measurement on samples etched 0.25, 0.5 and 0.75  $\mu\text{m}$  with a phosphoric acid solution. The optical properties of the structures were studied using non-resonant photoluminescence excited with the 325 nm line from a He–Cd laser. The emitted light was dispersed using a 0.6 m focal length monochromator equipped with a 1200 lines/mm grating and detected by using a silicon photomultiplier tube (PMT) with

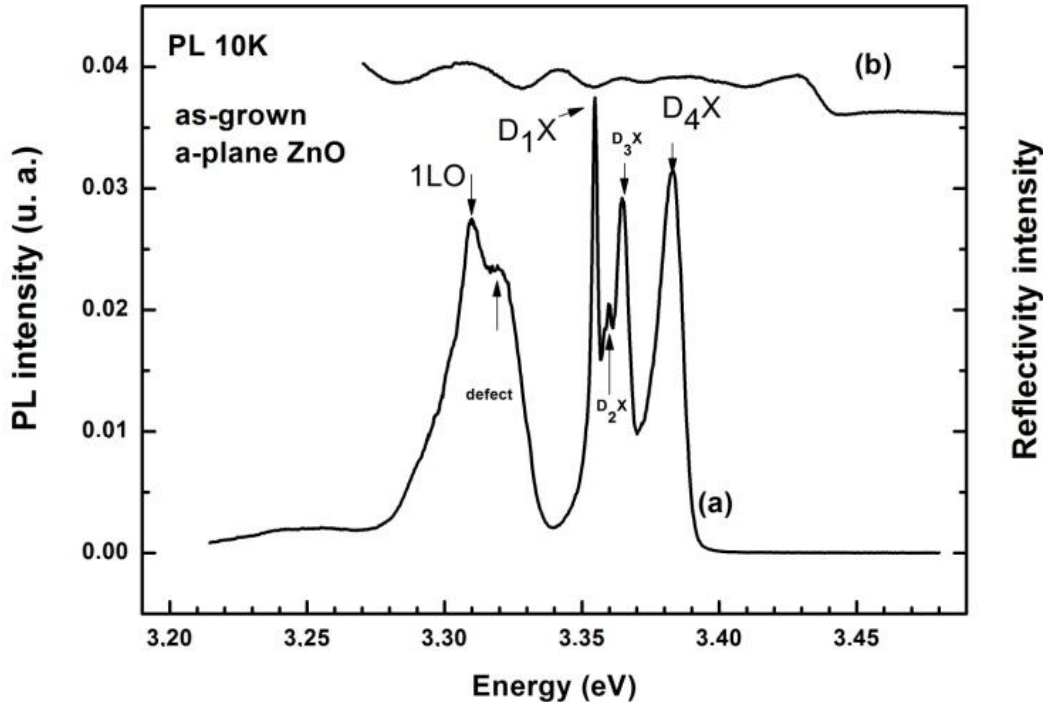


**Figure 1.** (a) Photoluminescence spectrum at 10K of as grown *a*-plane ZnO films and (b) Reflectivity spectrum at 10K of as grown *a*-plane ZnO film.

conventional lock-in techniques. The chopping frequency was set at 220 Hz. The sample was mounted in an optical cryostat where the temperature could be varied from 10 to 300 K. Reflectivity measurements were obtained by exciting using a standard mercury bulb. PL and reflectivity studies were performed on the samples at 10K.

## RESULTS AND DISCUSSION

Non-selective PL spectra and reflectivity of the as-grown ZnO film are both displayed in Figure 1. In this unpolarized measurements, PL emissions are seen in the energy ranges 3.35 to 3.41 eV, 3.28 to 3.35 eV.

It is difficult in the photoluminescence spectrum to distinguish the free excitons peaks in ZnO films because these excitons have approximate energies and large non-radiative damping constants. For these reasons, it is necessary to study the excitonic emissions of ZnO films in detail by using reflectivity for the determination of the peak position. The reflectivity spectrum allows distinguishing the free exciton peak positions and we found in the reflectivity spectrum the free excitons at energy positions higher than 3.38 eV. These free excitons are not resolved in the PL spectrum measured at 10K. This is due to the preeminence of the bound excitons.

Based on the assignment of the free excitons energy

peak, the bound excitons are the lines on the lower side energy range 3.35 to 3.395 eV. An emission was also identified lying in the first longitudinal optical phonon (LO) region, as defect resulting from the formation of basal stacking faults (Chauveau et al., 2007; Lim and Shindo, 2002). The bound excitons are labeled  $D_1X$ ,  $D_2X$ ,  $D_3X$  and  $D_4X$ .

In order to study the influence of the chemical etching, we studied the evolution of these peaks as the etching profile is increasing. The profile etching dependent PL (0.25 to 0.75  $\mu\text{m}$ ) was measured at 10K as shown in Figure 2. It is observed that the intensity of the peak attributed to the bound excitons exhibit similar dependence on the etching profile. The intensities of the peaks in the PL spectra from the samples etched were increased compared with the as-grown ZnO layer. However, as the etching profile increases, the intensity of the PL spectra started to decrease. This behavior is attributed to the decrease in the surface-to-volume ratio of the ZnO layers that resulted in the decrease of the PL band-edge intensity.

The intensity of the bound excitons decreases up to 0.75  $\mu\text{m}$  etching profile. The bound excitons  $D_2X$ ,  $D_4X$  disappear at 0.25  $\mu\text{m}$  etching profile whereas the first longitudinal optical phonon (LO) replica appears clearly as shown in Figure 3. The concomitant disappearing of the bound exciton  $D_4X$  and appearing of the (LO) replica

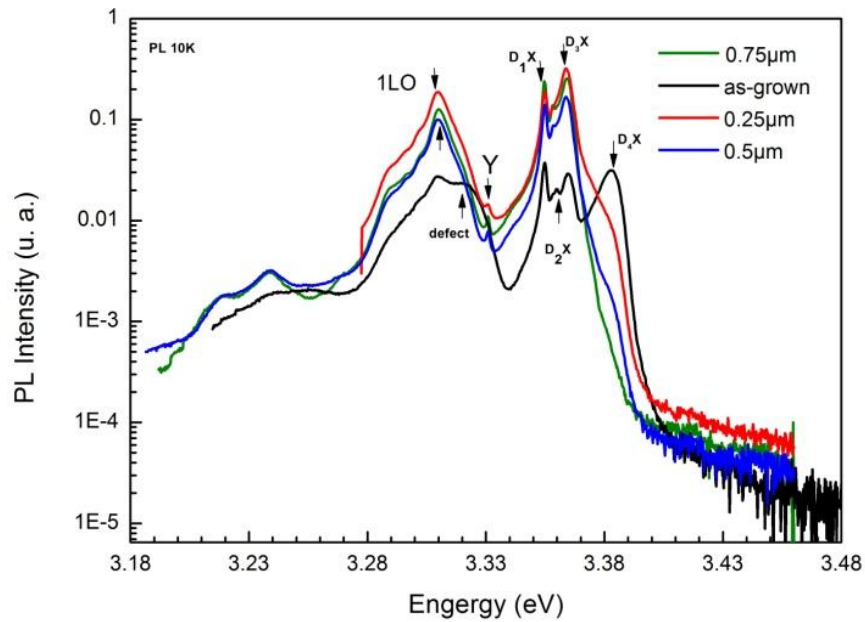


**Figure 2.** Photoluminescence spectra at 10K of as-grown and etched a-plane ZnO films from to 0.25 to 0.75 µm etching profile.

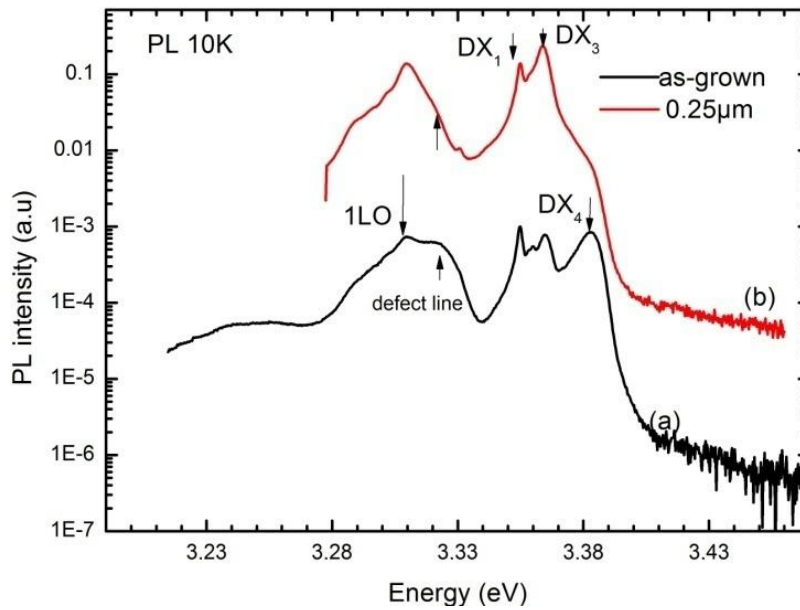


**Figure 3.** (a) Photoluminescence spectrum at 10K of as grown a-plane ZnO film and (b) Photoluminescence spectrum at 10K of a-plane ZnO films after 0.25 µm etching profile.

means that the free excitons peaks emission are overlapped by those of the bound exciton in the PL spectrum. We note that the defect line emission remains at the region of first longitudinal optical phonon (LO)

replica but its intensity is drastically decreased.

The intensity of the bound exciton  $D_1X$  and  $D_3X$  decreases further at 0.5 µm etching profile, whereas the intensity of the bound exciton  $D_2X$  become detectable.

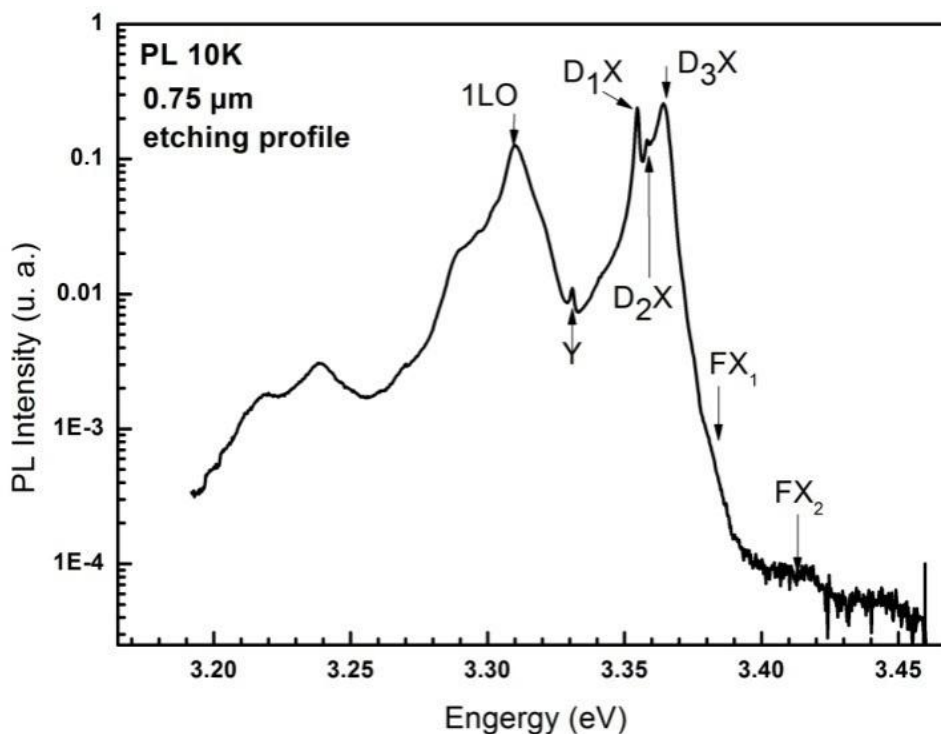


**Figure 4.** Photoluminescence spectrum at 10K of *a*-plane ZnO films after 0.75  $\mu\text{m}$  etching showing the free excitons  $\text{FX}_1$  and  $\text{FX}_2$  with more resolution.

This effect is attributed to the change in the chemical behavior of the ZnO sample. The etching influences the oxygen and Zn content in the sample. Furthermore an emission line appears at 3.33 eV, identified as the Y line, a characteristic of high quality ZnO samples. Also, the resolution of the free exciton peak emission is enhanced. Above 0.75  $\mu\text{m}$  etching profile, the  $\text{D}_2\text{X}$  bound exciton reappears clearly whereas the intensity of the bound excitons  $\text{D}_1\text{X}$  and  $\text{D}_3\text{X}$  increase a little bit and the free exciton emission  $\text{FX}_1$  has less resolution. These observations support the assignment that the donors  $\text{D}_1$  and  $\text{D}_3$  are related respectively to In and Al atoms (Morhain et al., 2002). When the etching profile increases, Al atoms can diffuse out easily from the sapphire substrate ( $\text{Al}_2\text{O}_3$ ) leading to increase in the intensity of the  $\text{D}_3\text{X}$  bound exciton. Also the lack of Zinc atom and oxygen atom can explain the enhancement of the bound exciton emission  $\text{D}_1\text{X}$  and  $\text{D}_2\text{X}$ . So these bound excitons are expected to be related interstitial defect or vacancies (Özgür et al., 2005).

At 0.75  $\mu\text{m}$  etching profile, we observe the enhancement of the excitons emission. So the free exciton emission the  $\text{FX}_2$  appears and providing that the optical properties of the ZnO sample are preserved and enhanced. The PL spectrum ZnO film at 0.75  $\mu\text{m}$  etching profile is displayed in Figure 4.

## Conclusion

In summary, we have investigated the etching dependent photoluminescence of undoped *a*-plane ZnO. Our results indicate that the optical properties of the ZnO sample are preserved and enhanced. At 0.75  $\mu\text{m}$  etching profile, we have identified two free excitons transitions  $\text{FX}_1$  and  $\text{FX}_2$ , so called respectively A-free exciton and B-free exciton. These excitons are not observable in the PL spectrum of the as-grown sample. Our results also demonstrate that the free excitons in *a*-plane ZnO conserve the blue shift in comparison to those of conventional *c*-plane material. Finally, the strong emission observed in the region of the 1LO phonon related to defects, as already confirmed, disappears above 0.5  $\mu\text{m}$  etching profile.

## Conflict of Interests

The authors have not declared any conflict of interests.

## REFERENCES

- Bagnall DM, Chen YF, Zhu Z, Yao T, Koyam S, Shen MY, Goto T (1997). Optically pumped lasing of ZnO at room temperature. *Appl. Phys. Lett.* 70 (17):2230.

- Brenner TM, Thomas A.F , Paul FN , Erich PM , Gang C , Dana CO, Thomas EF , Reuben TC (2014). Etch-Resistant Zn<sub>1-x</sub>Mg<sub>x</sub>O Alloys: An Alternative to ZnO for Carboxylic Acid Surface Modification. *J. Phys. Chem. C*.118 (24):12599-12607.
- Cao H, Zhao YG, Ong HC, Ho ST, Dai JY, Wu JY, Chang RPH (1998). Ultraviolet lasing in resonators formed by scattering in semiconductor polycrystalline films. *Appl. Phys. Lett.*73:3656.
- Chang SC, Hicks DB, Laugal RCO (1992). Patterning of zinc oxide thin films. *Solid-State Sensor Actuator Workshop (New York: IEEE)*. pp. 41-45.
- Chauveau JM, Morhain C, Lo B, Vinter B, Vennéguès P, Laügt M, Buell D, Tesseire-Doninelli M, Neu G (2007). Growth and characterization of A-plane ZnO and ZnCoO based heterostructures. *Appl. Phys. A* 88 (1):65-69.
- Ching CG, Leonard L, Ang CI, Ooi PK, Ng SS, Hassan Z, Hassan HA (2013). Effects of the Nitric Acid Concentrations on the Etching Process, Structural and Optical Properties of Porous Zinc Oxide Thin Films. *Sains Malaysiana* 42(9):1327-1332.
- Ding P, Xinhua P, Jingyun H, Bin L, Honghai Z, Wei C, Zhizhen Y (2012). Growth of p-type a-plane ZnO thin films on r-plane sapphire substrates by plasma-assisted molecular beam epitaxy. *Mater. Lett.* 71:18-20.
- Fernández S, De Abril O, Naranjo FB, Gandía JJ (2011). High quality textured ZnO: Al surfaces obtained by a two-step wet-chemical etching method for applications in thin film silicon solar cells. *Sol. Energy Mater. Sol. Cells* 95(1):2281-2286.
- Han SK, Soon-Ku H, Jae WL, Jae GK, Myoung-ho J, Jeong YL, Sun I , Jin SP, Young EI , Jun-Seok H , Takafumi Y (2011). Properties of (11-20) a-plane ZnO films on sapphire substrates grown at different temperatures by plasma-assisted molecular beam epitaxy. *Thin Solid Films* 519(19):6394-6398.
- Ipa K., Overberg ME, Baik KW, Wilson RG, Kucheyev SO, Williams JS, Jagadish C, Rend F, Heo YW, Norton DP, Zavadae JM, Pearton SJ (2003). ICP dry etching of ZnO and effects of hydrogen. *Solid-State Electron.* 47:2289-2294.
- Ito Y, Kushida K, Sugawara K, Takeuchi H (1995). A 100-MHz ultrasonic transducer array using ZnO thin films. *IEEE Trans. Ultrason. Ferroelectr. Freq. Control* 42(2):316-324.
- Jingchang SJB, Hongwei L, Jianze Z, Lizhong H, Ziwen Z, Weifeng L, Guotong D ( 2007). Realization of controllable etching for ZnO film by NH<sub>4</sub>Cl aqueous solution and its influence on optical and electrical properties. *Appl. Surf. Sci.* 253(11):5161-5165.
- Jong-Chang W, Tae-Kyung H, Chen L, Seung-Han K, Jung-Soo P (2011). *Transactions on electrical and electronic materials. The Korean Institute of Electrical and Electronic Material Engineers* 12(2):51-55.
- Liang Y (2010). Growth and characterization of nonpolar a-plane ZnO films on perovskite oxides with thin homointerlayer. *J. Alloys. Compd.* 508(1):158-161.
- Lim SH, Shindo D (2002). High-resolution electron microscopy of stacking faults in heteroepitaxial ZnO/LiTaO<sub>3</sub>. *J. Electron Microsc.* 51:165-169.
- Look DC (2001). Recent advances in ZnO materials and devices. *Mater. Sci. Eng.* 80(1-3):383-387.
- Lou KC, Zhu X, Lakdawala H, Kim ES (1997). Study on etch front of piezoelectric ZnO film and new step coverage technique. *Ultrason. Symp.* 1:565-568.
- Maki H, Ikoma T, Sakaguchi I (2002). Control of surface morphology of ZnO (0001) by hydrochloric acid etching. *Thin Solid Films* 411(1):1-176.
- Morhain C, Tesseire M, Vézian S, Vigué F, Raymond F, Lorenzini P, Guion J, Neu G, Faurie J-P (2002). Spectroscopy of Excitons, Bound Excitons and Impurities in h-ZnO Epilayers. *Phys. Status Solidi (b)* pp. 881-885.
- Özgür Ü, Ya Al, Liu C, Teke A, Reshchikov MA, Doğan S, Avrutin V, Cho S-J, Morkoç H (2005). A comprehensive review of ZnO materials and devices. *J. Appl. Phys.* 98(4):041301
- Prasad M, Sahula V, Khanna VK (2013). ZnO Etching and Micro tunnel Fabrication for High-Reliability MEMS Acoustic Sensor. *Device and Materials Reliability, IEEE Transactions.* 14(1):545-554.
- Sun K, Yuanyuan VL, David BSJ, Thomas NJ (2014). pH-Controlled Selective Etching of Al<sub>2</sub>O<sub>3</sub> over ZnO. *Appl. Mater. Interfaces.* 6(10):7028-7031.
- Yu P, Tang ZK, Wong GKL, Kawasaki M, Ohtomo A, Koinuma H, Segawa Y (1997). Ultraviolet spontaneous and stimulated emissions from ZnO microcrystallite thin films at room temperature. *Solid State Commun.* 103(8):459-463.
- Zhang XT, Liu YC, Zhi ZZ, Zhang JY, Lu YM, Shen DZ, Xu W, Fan XW, Kong XG (2002). Temperature dependence of excitonic luminescence from nanocrystalline ZnO films. *J. Lumin.* 99(2):149-154.
- Zheng MJ, Zhang LD, Li GH, Shen WZ (2002). Fabrication and optical properties of large-scale uniform zinc oxide nanowire arrays by one-step electrochemical deposition technique. *Chem. Phys. Lett.* 363(1-2):123-128.
- Zhu J, Emanetoglu NW, Chen Y, Yakshinskiy BV, Lu Y (2004). Wet-chemical etching of (11 $\bar{2}$ 0) ZnO films ZnO films, Wet-chemical etching of (11 $\bar{2}$ 0) ZnO films ZnO films, *J. Electron. Mater.* 33(6):556-559.